**Radboud Repository**

Radboud University Nijmegen

# PDF hosted at the Radboud Repository of the Radboud University Nijmegen

The following full text is a publisher's version.

For additional information about this publication click this link.
http://hdl.handle.net/2066/98848

Please be advised that this information was generated on 2017-12-06 and may be subject to change.

# Resonant infrared laser-induced desorption of methane condensed on NaCl(100): Isotope mixture experiments

Britta Redlich
*FOM Institute for Plasma Physics Rijnhuizen, P.O. Box 1207, 3430 BE Nieuwegein, The Netherlands*

Helmut Zacharias[a]
*Westfälische Wilhelms-Universität Münster, Wilhelm-Klemm-Strasse 10, 48149 Münster, Germany*

Gerard Meijer and Gert von Helden
*Fritz-Haber-Institut der Max-Planck-Gesellschaft, Faradayweg 4-6, 14195 Berlin, Germany*

Resonantly enhanced infrared laser-induced desorption of methane condensed on a single-crystal NaCl(100) surface is observed after excitation with the widely tunable infrared laser output of the free-electron laser at the free-electron laser for infrared experiments facility using mass spectroscopic detection and time-of-flight analysis. Desorption of methane is observed only when the exciting light is in resonance with an internal vibrational mode of the molecule. Different intramolecular modes of the three methane isotopologues under study—$CH_4$, $CD_4$, and $CD_3H$—are excited; the degenerate deformation mode $\nu_4$ is observed for $CH_4$ and $CD_4$ at 7.69 and 10.11 $\mu$m, respectively, as well as the $\nu_2$ and $\nu_4$ modes of $CD_3H$ at 7.79, 9.75, and 9.98 $\mu$m. The desorption signals for the pure layers of these different methane isotopologues as well as for different mixtures of two of these are investigated as a function of the infrared wavelength and the laser fluence. The desorption behavior for pure and mixed layers is compared and the underlying desorption mechanism is discussed. © *2006 American Institute of Physics.* [DOI: 10.1063/1.2159487]

## INTRODUCTION

One of the goals of the studies on vibrational modes of adsorbates or condensates on surfaces is to gain a better understanding of their role in energy transfer and dissipation processes, as well as in chemical reactions on surfaces. In this field it has been shown that surface processes such as desorption from insulating or metal surfaces can be induced by excitation of internal vibrations of adsorbed molecules in the electronic ground state.[1–8] For efficient resonant excitation of a vibrational mode, a pulsed tunable infrared laser source has to be employed. Recently it has been shown that a free-electron laser (FEL) operating in the infrared is a well-suited radiation source for this kind of investigations.[9–11] Theoretical studies of desorption by laser-adsorbate vibrational coupling and energy transfer have been carried out,[12–17] particularly for the well-investigated physisorption system CO/NaCl(100).[18,19]

In the present work the infrared laser-induced desorption of different methane isotopologues condensed on a NaCl(100) single-crystal surface is investigated using the FEL of the free-electron laser for infrared experiments (FELIX) facility in the Netherlands as the excitation source. The present study is beginning to explore the field of mode and isotope selectivity after resonant infrared excitation of vibrational modes in condensed layer systems on dielectric surfaces. Considering different isotopologues the question arises whether the different IR-active modes such as bending and stretching modes can lead to a significantly different desorp-

tion behavior. The density of states accessible for further excitation is increased for larger systems after resonant excitation and one can ask how this influences the desorption process, e.g., due to coupling of intra- and intermolecular modes. Besides the mode selectivity also the isotope selectivity sheds light on the underlying mechanism of the desorption process. Isotope selectivity is only expected in cases of resonant excitation followed by a direct desorption step or when energy scrambling between different adsorbates is prohibited. The former is possible when the energy deposited in a specific mode exceeds the binding energy of the molecule within the layer or to the substrate and rupture of this bond occurs. In case no selectivity is observed for the desorption process, the desorption involves either a resonant heating mechanism leading to thermal desorption, a *V-V* transfer process among the species, followed by vibrational energy transfer from the internal vibrational mode to the desorption coordinate of the adsorbed molecule, or a collisional interaction within the adsorbate in dense systems. In general, the dynamics of the desorption process will depend on the coupling and the energy flow between the different degrees of freedom.

## EXPERIMENT

The experiments are performed in a standard ultrahigh-vacuum (UHV) chamber using the infrared light output of the FEL of the FELIX facility at our Institute.[20] The infrared radiation produced by the FEL is continuously tunable between 5 and 250 $\mu$m, and the wavelength ranges between 3 and 5 $\mu$m can be accessed by operation on the third har-

monic. For the desorption experiments presented here, the wavelength regimes from 7 to 12 $\mu$m and from 3.25 to 3.4 $\mu$m are used. The infrared light is pulsed and consists of so-called macropulses that are on the order of 5 $\mu$s long and that having a repetition rate of 5 Hz. A macropulse contains a series of micropulses that are equally spaced by 1, 20, or 40 ns. The experiments presented are performed in the 1 GHz operation mode corresponding to a micropulse spacing of 1 ns. The micropulse duration depends on the laser settings and is adjustable in duration between a few hundred femtoseconds and several picoseconds. For the desorption experiments the spectral bandwidth, which is Fourier transform limited, is an important parameter. For these measurements, it is kept constant to about 0.5% full width at half maximum (FWHM) of the central frequency of the laser light or to about $4-7$ cm$^{-1}$, which corresponds to a pulse duration of about $2-3$ ps. Macropulse energies can reach up to 100 mJ, but typical pulse energies at this wavelength range and bandwidth are on the order of 20 mJ at the experiment. Correspondingly, the energy in a micropulse is typically of the order of 4 $\mu$J. Values reported for the laser energy are measured directly in front of the KBr entrance window to the UHV chamber. The laser fluence is varied either using attenuators or by changing the size of the laser spot on the surface with a KBr lens ($f=470$ mm). The angle of incidence for the $\hat{p}$-polarized laser light onto the surface is 45° with respect to the surface normal.

The NaCl(100) single crystal ($20\times20\times3$ mm$^3$, purity of 99.99%) is cleaved *ex situ* under dry nitrogen atmosphere and is immediately transferred to the vacuum chamber. It is mounted to a copper sample holder, which is connected to a manipulator constructed for low-temperature application. The sample can be cooled to 25 K using liquid helium. Between the experiments, the sample is maintained at 450 K to avoid contamination, especially adsorption of water onto the surface. The sample temperature is controlled using two thermocouple pairs (NiCr–Ni and AuFe–Cr) attached to the sample holder. The sample can be manipulated in $x$, $y$, and $z$ directions, rotated polarly by 360°, and tilted azimuthally, which enables precise positioning with respect to the laser beam.

The cryostat and manipulator are mounted in a standard UHV chamber operated at a base pressure of $2\times10^{-10}$ mbar. Both the entrance and the exit windows are made of KBr to minimize the influence of light scattered inside the chamber. The UHV apparatus is equipped with a sensitive, differentially pumped quadrupole mass spectrometer (Extrel Q50). The neutral species desorbing from the surface are detected mass selectively using electron-impact ionization and a channeltron detector. The direction of the detection is normal to the surface plane. The distance between the surface and the electron-impact ionizer is 16 cm. The mass-selected signal is recorded as a function of time after the laser pulse.

The condensed layers of the different methane isotopes (CH$_4$ from Messer Griesheim 99.995%, CD$_3$H and CD$_4$ from Cambridge Isotope Laboratories Inc. D-98% and D-99%, respectively) are prepared at low temperature under nonequilibrium conditions via background dosing using a

leak valve. The adsorption temperature is chosen low enough to ensure that on the time scale of the experiment no significant thermal desorption occurs. The gas inlet is made of stainless steel and operates at a base pressure of $1\times10^{-6}$ mbar; no further purification of the gas is carried out. Typically a few hundred monolayers (ML) are condensed using gas pressures on the order of $1\times10^{-6}$ mbar. At these coverages a fairly homogeneous irradiation of the layer is still ensured. For a 500-ML-thick methane film on resonance, about 55% of the IR radiation is transmitted. The coverage is estimated using a sticking coefficient of 1. In addition, a Fourier transform infrared (FTIR) spectrometer (Bruker IFS66v) is attached to the UHV chamber, which allows to record FTIR spectra in transmission geometry with a liquid-nitrogen-cooled mercury-cadmium-telluride (MCT) detector. Analysis of the integrated absorption enables a cross-check of the coverage.

## RESULTS

The feasibility to study infrared laser-induced desorption of small molecules from insulator surfaces using the FEL at the FELIX facility as an infrared radiation source was shown for CD$_3$F and N$_2$O condensed on NaCl(100).[9–11] In the present investigation, we report results on desorption experiments of methane condensed on NaCl(100). Experiments are performed with three methane isotopologues—CH$_4$, CD$_4$, and CD$_3$H—as well as with mixed layers of these isotopes.

### Pure isotopes

At a temperature of 25 K, layers of CH$_4$, CD$_4$, or CD$_3$H with a thickness of about 500 ML are condensed onto a NaCl(100) single-crystal surface. The mass-selected ion signal for the respective isotope is recorded as a function of the FELIX wavelength in the range between 7 and 12 $\mu$m. For the pure isotopes the primary peak is used for mass-selective detection (CH$_4$: 16 amu, CD$_4$: 20 amu, and CD$_3$H: 19 amu). The mass spectra of the desorbing species show a fragmentation pattern similar to the ones known for gas-phase molecules, indicating desorption of neutral and intact molecules. Figure 1(a) shows the desorption spectra of the pure isotope systems for an IR fluence between 1.5 and 2.2 J/cm$^2$ per macropulse. At these fluences between a fraction and a few monolayers are desorbed per macropulse. For each isotope desorption is observed only at specific infrared wavelengths: CH$_4$ at 7.69 $\mu$m (1300 cm$^{-1}$), CD$_4$ at 10.11 $\mu$m (989 cm$^{-1}$), and CD$_3$H at 7.79 (1284 cm$^{-1}$), 9.75 (1026 cm$^{-1}$), and 9.98 $\mu$m (1002 cm$^{-1}$). These wavelengths show that resonant excitation of the first internal vibrational modes in the molecules occurs. In the spectral range studied here there is no detectable desorption signal at frequencies other than the ones mentioned, even at the highest laser fluences applied. The corresponding linear absorption spectra recorded with a FTIR spectrometer are shown in Fig. 1(b) for comparison. The spectra are taken under comparable experimental conditions at a sample temperature of 25 K and for a coverage of 1000 ML. The spectral resolution is 0.5 cm$^{-1}$. The absorption spectra are obtained by division of a sample spectrum by a reference spectrum, which was recorded for the uncovered
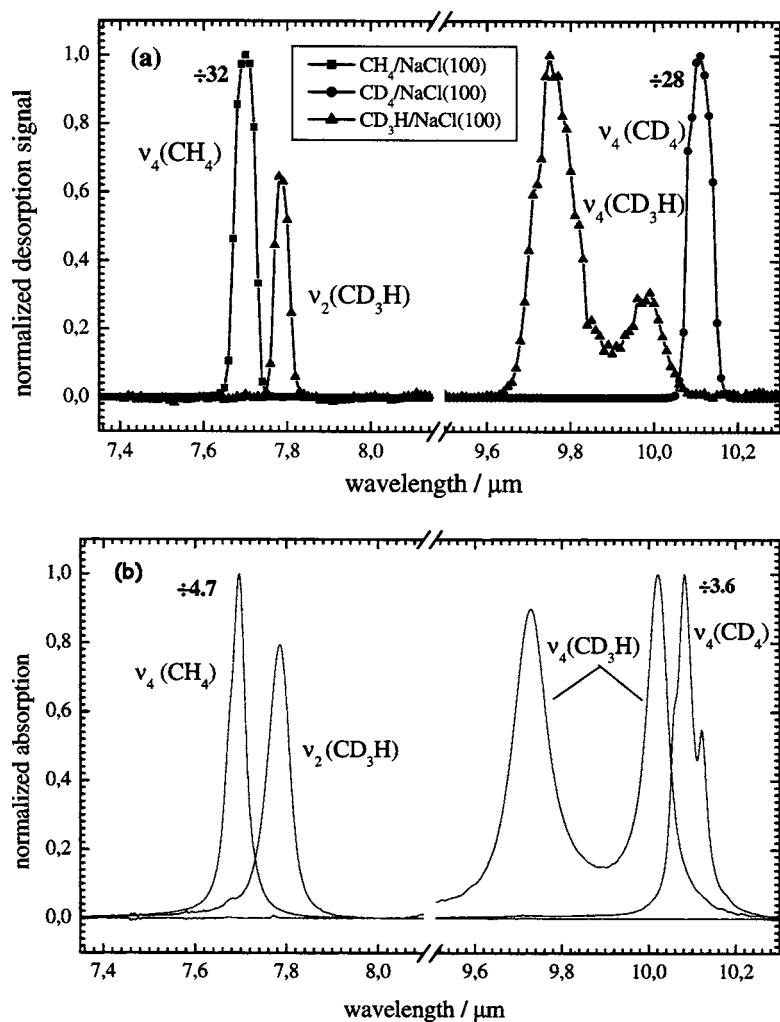
FIG. 1. (a) Laser-induced desorption spectra of the methane isotopes $CH_4$, $CD_3H$, and $CD_4$ condensed on NaCl(100) using FELIX (step size of 0.01 $\mu$m) at an IR fluence of 1.5–2.2 J/cm$^2$, detected on masses 16, 19, and 20, respectively. (b) Linear absorption spectra for the same systems recorded with a FTIR spectrometer (resolution of 0.5 cm$^{-1}$). The spectra are recorded for a layer thickness of 500 ML for the desorption case and 1000 ML for the linear absorption case at a temperature of 25 K. For a better comparison of frequencies and bandwidths, the most intense absorption peaks in the individual spectra are normalized to one. Relative intensities at the peaks are indicated.

surface at the measurement temperature of 25 K. The spectra exhibit the absorption bands of the condensates $CH_4$, $CD_4$, and $CD_3H$, which are labeled according to convention.[21]

Comparing the desorption spectra to the linear absorption spectra, a clear correspondence is found. Frequencies and bandwidths of the peaks are observed to be identical in both sets of spectra within the experimental error. The only exception is the $\nu_4$ mode of $CD_3H$, which splits in both cases into two components, but the observed splitting is slightly different. In the desorption case the modes are observed at 9.75 $\mu$m (1026 cm$^{-1}$) and 9.98 $\mu$m (1002 cm$^{-1}$), while for the linear absorption spectrum the peak maxima are found at 9.73 $\mu$m (1028 cm$^{-1}$) and 10.02 $\mu$m (998 cm$^{-1}$). A systematic error is unlikely since the frequency shift is opposite for the two components. However, since the spectra are not recorded for the same layer and coverage, small differences in the preparation procedure might cause this change in splitting. Nevertheless, it can be concluded that desorption is observed only if the infrared laser excitation is in resonance with an internal vibrational mode of the methane isotope. Nonresonant desorption is not observed.

For $CH_4$ and $CD_4$ the relative intensities compare well for absorption and desorption. In linear absorption the integrated intensities of the $\nu_4$ bands yield ratios of 0.97:1.00 for $CH_4$:$CD_4$ [Fig. 1(b)]. In desorption the symmetric isotopes yield ratios of 0.99:1.00. The situation is very different for

the asymmetric isotope $CD_3H$. The integrated intensity of the splitted $\nu_4$ band amounts in desorption to only 9% of that of $CD_4$ while in absorption a relative intensity of 82% is measured. From the data one could conclude that the two components of the $\nu_4$ band show different efficacies for desorption, but as discussed in more detail later on the effect can mainly be attributed to the way of data acquisition. Finally, the widths of the spectral features may be mentioned. For $CH_4$ and $CD_4$ again similar results are obtained in desorption and linear absorption with respective values of 8.5 and 7.2 cm$^{-1}$ for $CH_4$ and correspondingly of 6.8 and 5.3 cm$^{-1}$ for $CD_4$. $CD_3H$ behaves now similar to the other isotopes. In desorption the spectral widths are 6.6 cm$^{-1}$ for the $\nu_2$ band and 12.6 and 10.0 cm$^{-1}$ for the high- and low-frequency component of the $\nu_4$ band. In absorption the corresponding values are 9.2, 10.5, and 6.0 cm$^{-1}$, respectively.

Figure 2 shows the dependence of the desorption signal on the applied laser fluence after resonant excitation of the $\nu_4$ mode of $CH_4$, $CD_4$, and $CD_3H$ ($\lambda$=7.69, 10.11, and 9.75 $\mu$m), respectively. Day-to-day differences in the operating conditions of the FEL cause the variability in the laser fluences applied to study the desorption yield of the individual isotopes. The overall dependence of the desorption signal for this mode is similar for the different isotopes. For $CH_4$ and $CD_4$ a measurable desorption yield can be observed only at fluences above 0.5 J/cm$^2$, while for $CD_3H$ signifi-
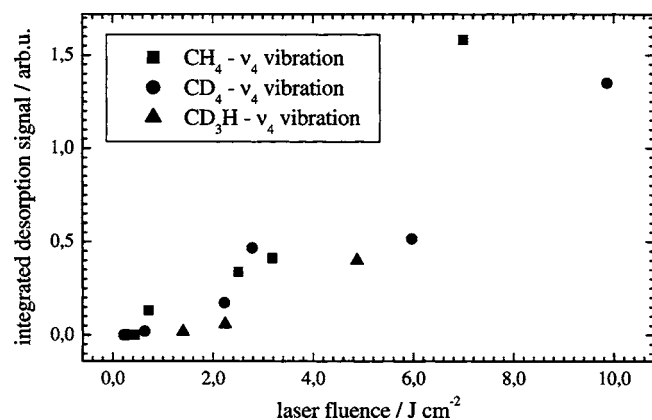
FIG. 2. Dependence of the desorption signal on the laser fluence for multi-layers of $CH_4$, $CD_4$, and $CD_3H$ condensed on NaCl(100) after resonant excitation of the $\nu_4$ mode at 7.69, 10.11, and 9.75 $\mu$m, respectively.

cantly higher laser fluences of more than 1.5 J/cm$^2$ have to be applied. For all three isotopes the desorption signal shows a slightly nonlinear dependence on the fluence.

The time-of-flight (TOF) spectra of the different isotopes excited at the resonance frequency of the $\nu_4$ mode are shown in Fig. 3. The resulting velocity distribution has therefore been fitted with a modified Maxwell distribution of the form

$$f(t) = \frac{a}{t^3} \exp\left(-\frac{m}{2kT}\left(\frac{d}{t} - u\right)^2\right),$$

where $d$ denotes the distance from the surface to the detector, $u$ is the stream velocity, and $a$ is a normalization factor. For clarity the results of these fits to the TOF distributions are not included in the figure. The fits show that the leading slope, the maximum of the flight-time distribution, and the beginning of the falling tail can be well described with a thermal velocity distribution; due to insufficient differential pumping capabilities in the setup, the signal decreases slower than expected for a Maxwellian distribution for later times. The fits yield the maxima of the TOF distributions at the times indicated in Fig. 3. These times scale with the square root of the mass as expected for the most probable velocity resulting
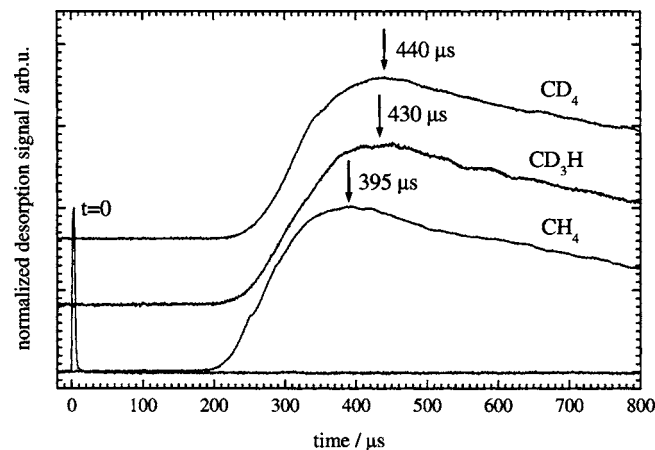


FIG. 3. Time-of-flight spectra for the desorption of $CH_4$, $CD_4$, and $CD_3H$ recorded at the resonance frequencies of the $\nu_4$ mode. The maxima of the flight-time distribution are indicated for each time-of-flight spectrum in the figure. The spectra are offset for clarity.
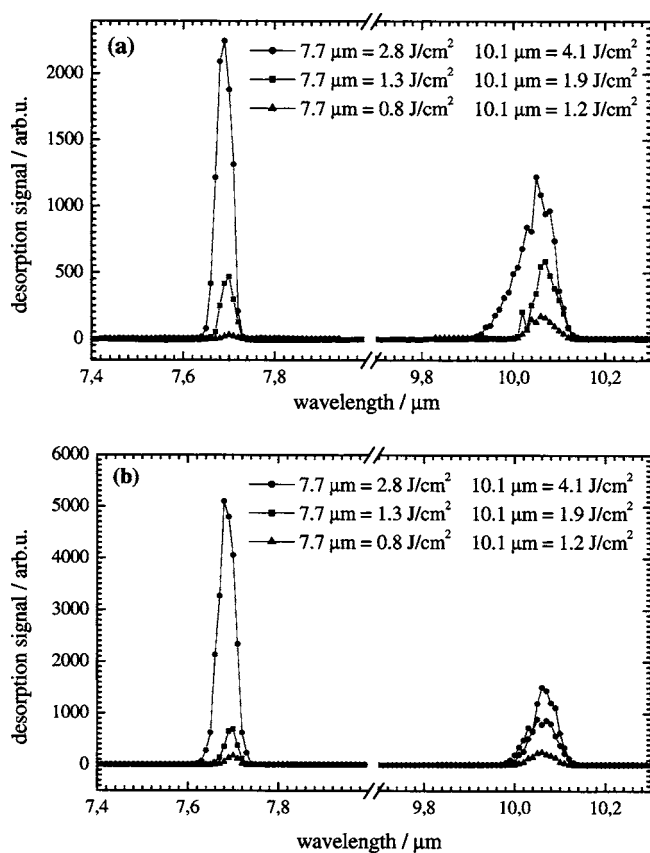


FIG. 4. Desorption spectra of isotopically mixed layers ($CH_4$:$CD_4$ =50:50) resonantly excited via the $\nu_4$ bending modes of the isotopes at 7.69 and 10.11 $\mu$m. The desorption yield for $CH_4$ (a) is monitored on mass 15 and for $CD_4$ (b) on mass 20 for different laser energies. Layer thickness and temperature are kept comparable during the experiments; the experimental parameters of FELIX are indicated.

from a Maxwell-Boltzmann distribution. The resulting translational temperatures are on the order of 40–50 K, i.e., well above the surface temperature of 25 K.

## Randomly mixed isotopes

In the following, experiments performed on different randomly mixed (50:50) multilayers of the three isotopes are described. During the series of measurements the experimental parameters such as thickness (300 ML), temperature (25 K), and the parameters of the FEL such as bandwidth and intensity are kept constant as much as possible. In the case of $CH_4$ and $CD_4$ both molecules exhibit only one infrared-active mode in the spectral range under investigation, the $\nu_4$ vibrations, which are spectrally well separated from each other by about 300 cm$^{-1}$. The molecules are detected on mass 15 for $CH_4$ and on mass 20 for $CD_4$.

The desorption yields are shown in Fig. 4(a) for the detection of $CH_4$ and in Fig. 4(b) for the detection of $CD_4$ at three different laser fluences, as indicated in the inset of Fig. 4. The laser fluence for the longer wavelength is higher by about 50% and the laser linewidth at those frequencies is slightly larger. Also for the mixed layers a desorption signal was observed only at the resonance frequencies independent of the exciting laser fluence. The observed frequencies are almost unchanged as compared to the pure systems. It is

evident that the excitation of the internal deformation vibration of one isotope also causes the other isotope to desorb. With increasing laser fluences a broadening of the desorption bands is observed.

Both molecules show a similar but nontrivial dependence of the desorption yield on the laser fluence. At low intensity the efficacy of the $CD_4$ $\nu_4$ vibration of desorbing either $CD_4$ or $CH_4$ seems to be higher than the corresponding $CH_4$ vibration despite its lower energy content (989 cm$^{-1}$ vs 1300 cm$^{-1}$). This behavior is reversed at high laser intensities. Moreover, excitation of the $CD_4$ vibration results in a nearly linear increase of the desorption yield with laser fluence irrespective of the desorbing molecule. On the other hand, excitation of the $CH_4$ vibration clearly shows a nonlinear increase of the desorption yield, again irrespective of the desorbing molecule. Finally, it can be noted that the yield of $CD_4$ is significantly higher—by a factor of 2—than for $CH_4$ when the system is excited on the $CH_4$ vibration. Looking carefully at all data it is also observed that the maxima of the desorption peaks shift with increasing laser fluence to shorter wavelength and that the peaks become asymmetric.

In another set of experiments isotope mixtures consisting of $CH_4$ and $CD_3H$ as well as mixtures of $CD_4$ and $CD_3H$ are investigated. These two systems are different from the mixture of $CH_4$ and $CD_4$ discussed before, because the absorption bands are not well separated anymore. For the mixture containing $CH_4$ they are almost overlapping around 7.7–7.8 $\mu$m and for the one with $CD_4$ around 10.0–10.1 $\mu$m. In Fig. 5 the desorption spectra are shown for different laser fluences for the mixture $CH_4$:$CD_3H$ =50:50 (a) detected on mass 15 for $CH_4$ and (b) detected on mass 19 for $CD_3H$. The mass channels for detection are selected such that the contribution from the other isotope is not existing or minimal. Also for this mixed system it is found that desorption of both isotopes occurs only after resonant excitation of one of the isotopes. For the $CH_4$ line again a blueshifted broadening is observed at high laser intensities. The two spectra measured do not depend on the detection channel. The efficacy of the $\nu_4$ vibration of $CD_3H$ is low, as can be expected from the pure isotope spectrum. More striking is the complete absence of the $\nu_2$ vibration of $CD_3H$, for desorption of $CH_4$ as well as for $CD_3H$ molecules, although the band is spectrally well separated (by 17 cm$^{-1}$) from the $CH_4$ line.

Figure 6 shows corresponding studies for the mixture $CD_4$:$CD_3H$=50:50 (a) detected on mass 16 for $CD_4$ and (b) detected on mass 19 for $CD_3H$. Mass channel 16 instead of 20 for the detection of $CD_4$ was an unfortunate choice. However, the only consequence is that the detection is less efficient by more than one order of magnitude, because mass 16 is a minor fragmentation channel of $CD_4$; the data in Fig. 6 are corrected for this difference. Now the $\nu_2$ vibration of $CD_3H$ is again active and is compared to the $\nu_4$ vibration with similar efficacy as in the pure isotope case. In all spectra shown in Figs. 4–6 the desorption yield shows a clear nonlinear dependence on laser-pulse energy, as is also expected from the results shown in Fig. 2.
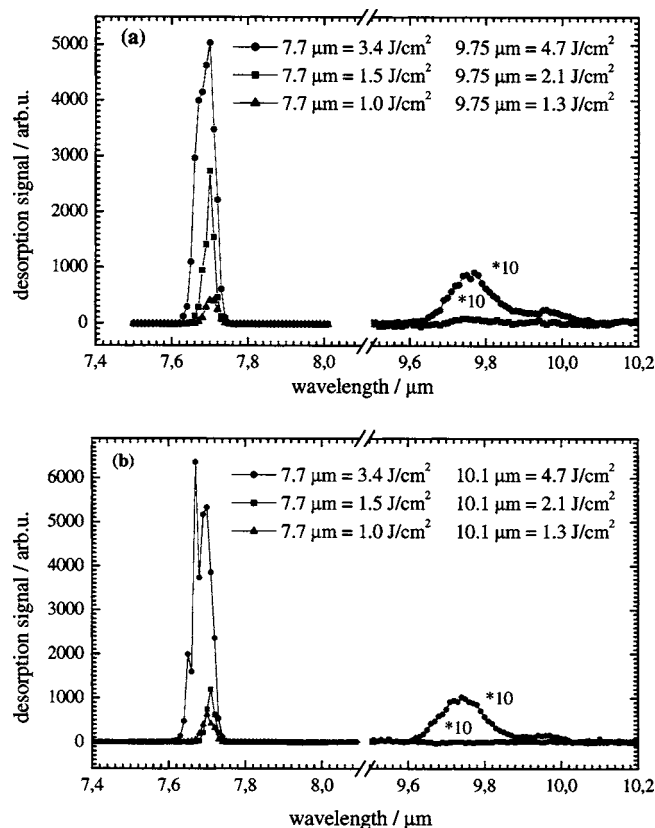


FIG. 5. Desorption spectra of randomly mixed layers of $CH_4$:$CD_3H$ =50:50 resonantly excited via the $\nu_4$ mode ($CH_4$) and the $\nu_2$ and $\nu_4$ modes ($CD_3H$). The desorption yield is monitored (a) on mass 15 for $CH_4$ and (b) on mass 19 for $CD_3H$ for different laser-pulse energies. Layer thickness and temperature are kept comparable during the experiment; the experimental parameters of FELIX are indicated.

## Layered isotopes

In a last set of measurements in experiment (1) 300 ML $CD_4$ was condensed on top of 300 ML $CH_4$ and in experiment (2) the order is reversed and 300 ML $CH_4$ was condensed on top of 300 ML $CD_4$. Figure 7(a) shows the corresponding FTIR spectra for experiments (1) and (2) for the first and second adsorption step in the spectral range of the $\nu_3$ and $\nu_4$ modes. This time, for the laser-induced desorption experiments, the FEL was operated on the third harmonic to enable excitation of the $\nu_3$ vibration of $CH_4$ at 3.33 $\mu$m (3003 cm$^{-1}$). In this mode of operation the tuning range is very restricted and it was only possible to excite the $\nu_3$ vibration of $CH_4$. The results are shown in Fig. 7(b). In experiment (1), where the $CH_4$ layer was covered by a $CD_4$ layer, desorption of $CH_4$ as well as of $CD_4$ was observed after excitation of $CH_4$. In contrast, in the case of experiment (2) where the $CH_4$ layer was condensed on top of the $CD_4$ layer, only desorption of $CH_4$ was found.

## DISCUSSION

The desorption spectra recorded for $CH_4$, $CD_4$, and $CD_3H$ condensed on NaCl(100) show desorption peaks only when the infrared wavelength is in resonance with an internal vibrational mode of the molecules. Therefore, it can be unambiguously concluded that the first step leading to the
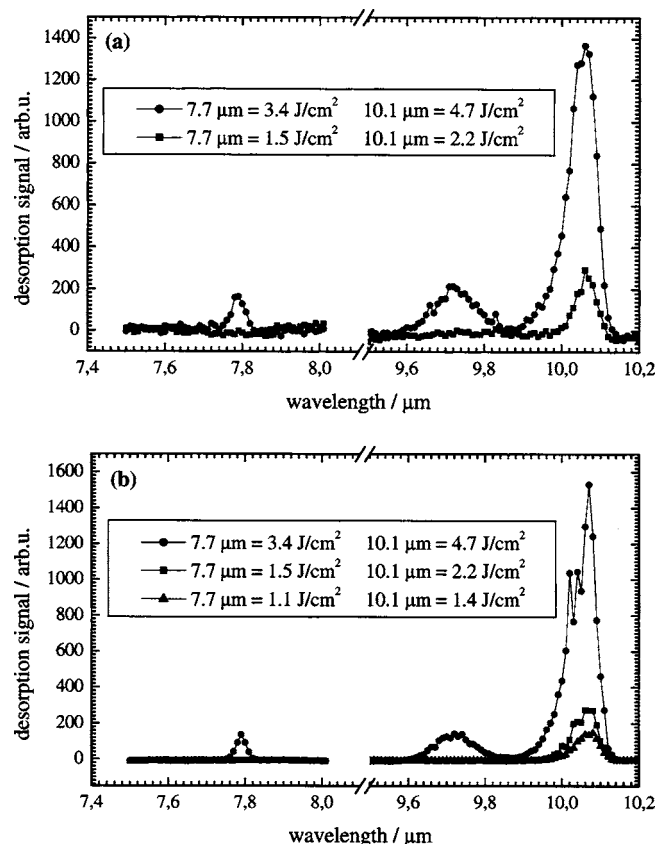
FIG. 6. Desorption spectra of randomly mixed layers of $CD_4$:$CD_3H$ $=50$:$50$ resonantly excited via the $\nu_4$ mode of $CD_4$ and the $\nu_2$ and $\nu_4$ modes of $CD_3H$. The desorption yield is monitored (a) on mass 16 for $CD_4$ and (b) on mass 19 for $CD_3H$. Different laser-pulse energies are indicated.

desorption process is resonant in character. A comparison of the desorption spectra to the linear absorption spectra shows identical behavior for the systems $CH_4$ and $CD_4$ concerning frequencies, linewidths, and relative and absolute intensities, suggesting therefore for both systems a very similar energy-flow and desorption processes after resonant excitation of the $\nu_4$ mode.

In contrast, the desorption spectra of $CD_3H$ show clear differences: The integrated desorption yield of the $\nu_4$ band is almost an order of magnitude lower than the corresponding bands in $CH_4$ and $CD_4$. The two peaks of the $\nu_4$ band show differences in the desorption efficacies as well as in their spectral separation when compared to the linear absorption spectrum. These observations are most likely explained by a desorption process requiring several photons for desorption. Given the fact that there is already, in the linear absorption spectrum, a considerable intensity difference of the two bands of $CD_3H$ and the symmetric isotopes $CH_4$ and $CD_4$, this can easily lead to a difference of an order of magnitude for the nonlinear case. While the slight differences in the splitting of the $\nu_4$ band for the linear and the desorption case can be readily explained with small differences in the layer, the different efficacies of the two peaks have a different origin. The scanning programs for the FEL permitted only to scan from shorter to longer wavelength and not reversed. This might, for thicker layers and at high intensities, lead to a situation where on the blue side of the band a significant fraction of the layer is desorbed before the red part of the band is reached. Since at higher fluences the bands appear to be broadened, the increased desorption on the blue wing appears like a blueshift of the peak and can also introduce an asymmetry in the line shape. However, besides this technical reason, additional contributions can also be discussed as, e.g., a different energy-loss mechanism not operative in the highly symmetric molecules or a different desorption mechanism for the $CD_3H$ molecule. Detailed investigations of the lifetimes and energy-flow processes are needed to clarify this point, and recently we started time-resolved measurements using pump-probe spectroscopy to test this hypothesis.

The desorption mechanism was further investigated by studying the dependence of the desorption signal on the laser fluence and by analyzing the TOF spectra of the different isotopes. The dependence of the desorption signal on the laser fluence is nonlinear for all three isotopes, which is an indication for a resonant heating process as desorption mechanism as can be shown from model calculations. Each individual micropulse causes a peak temperature rise of a few Kelvins, which is nearly completely dissipated before the next one arrives. The whole macropulse, however, causes a heating of the layer by several tens of Kelvin.[22] The analysis of the TOF spectra also points to a resonant heating process. For the three isotopes the change of the flight time is found to depend on the square root of the mass as expected when desorption occurs at a definite temperature and thus with a definite kinetic energy. The TOF spectra can be fitted using a modified Maxwell-Boltzmann distribution. The translational temperature of $40-50$ K obtained for all three isotopes is well above the substrate temperature and close to the thermal desorption temperature of condensed methane.

Experiments performed on different mixed layers of the three methane isotopes all show that desorption is observed after resonant excitation of one of the vibrational modes of one of the species contained in the layer. This proves once more the resonant character of the first step of the process also for these special layers. However, the desorption signal observed always consists of both isotopic components of the layer. For a direct desorption mechanism the desorption of the one component that is not resonantly excited should not occur or at least be diminished. The fact that there is no isotope selectivity observed in the desorption signal rules out the direct desorption and strengthens the assumption of a resonant heating mechanism as an underlying desorption process.

The dependence of the desorption signal from the mixed layers on the laser fluence can be understood when above a certain value of laser-pulse energy the amount of energy accumulated in the layer is high enough to reach the desorption temperature. Below this value no desorption is observable. Such a desorption would be in accordance with a resonant heating model of desorption. Once this value is reached desorption occurs and it is expected that the signal intensity then depends linearly on the laser fluence.

The last point to address in the series of measurements on mixed layers of methane isotopes is the situation of mixtures of $CH_4-CD_3H$ as well as of $CD_4-CD_3H$ where the vibrational modes of the different isotopes are not clearly
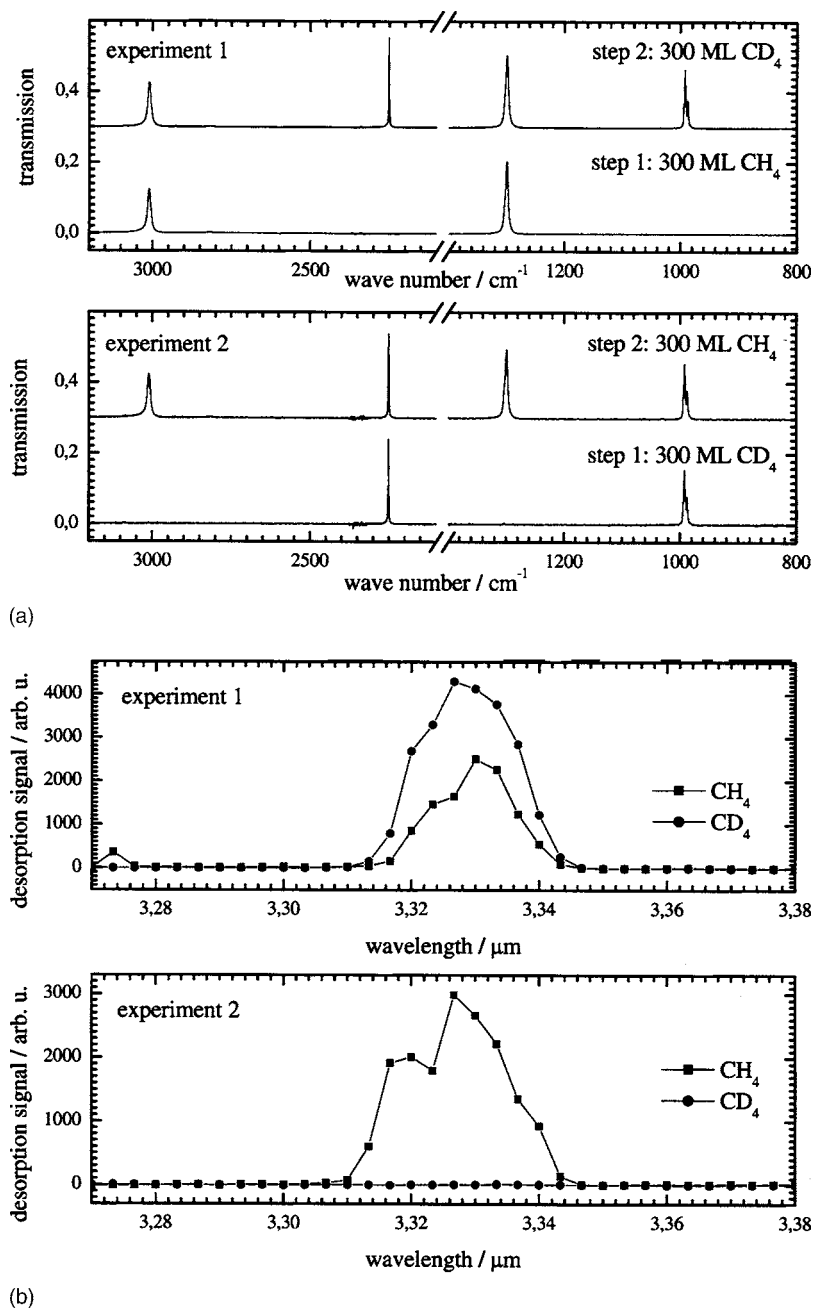
(a)

(b)

FIG. 7. (a) FTIR spectra of layers of $CH_4$ and $CD_4$ condensed on top of each other. In experiment (1) in a first step 300 ML $CH_4$ was condensed on NaCl(100) at 25 K and in a second step 300 ML $CD_4$ was condensed on top of the layer. In experiment (2) the order of condensation was reversed. The two graphs show the IR spectra of the layered systems recorded always after steps 1 and 2. (b) Desorption spectra from this layered system, recorded for detection of $CH_4$ as well as $CD_4$ after resonant excitation of the $\nu_3$ mode of $CH_4$ at 3.33 $\mu$m. In experiment (1) the excited $CH_4$ was beneath the $CD_4$ layer, in experiment (2) on top of $CD_4$.

separated but almost overlapping. In those cases it is observed that the weaker components in the overlapping regime, i.e., the $\nu_2$ mode of $CD_3H$ in the mixture with $CH_4$ and the lower-frequency component of the $\nu_4$ mode of $CD_3H$ in the mixture with $CD_4$, are not detectable as compared to the pure layer. The explanation for this observation is not readily clear. It is known from linear absorption spectroscopy that within mixed layers, intensity transfer can occur from the lower- to the higher-frequency mode due to shielding effects.[23] Such an effect would result in a reduction of the absorption coefficient and therefore it may be that the energy stored in the respective vibrational mode is not sufficient anymore to overcome the threshold value for desorption. To clarify this point unambiguously more detailed investigations are required.

The results observed for the layered methane isotopes yield yet another insight in the desorption mechanism. In experiment (1) the lower layer is resonantly excited and species from both layers are observed in the desorption flux. On the other hand when just the upper layer is excited, as in experiment (2), only molecules of this layer can be detected in the desorption flux. Thus the energy deposited in the layer via the resonant excitation remains locally confined.

Energy does not just flow to the top most layer causing these molecules then to desorb, because in that case one would observe only $CD_4$ molecules in experiment (1). Rather, in the laser-excited area the molecular constitutents acquire so much energy in the translational coordinate that they boil off from the solid. On their way out these molecules collide with other, not excited molecules and transfer in these collisions enough energy to cause the desorption of also these primarily nonexcited species. This mechanism can also explain the lack of isotopic selectivity in the randomly

mixed layers. Also the equilibrated kinetic energies of different isotopes can be established by such collisions.

## CONCLUSIONS

Infrared laser-induced desorption of multilayers of different methane isotopes and different mixtures of these isotopes condensed on NaCl(100) has been investigated. Desorption is observed only if the infrared excitation wavelength produced by the FEL is in resonance with one of the vibrational modes of the systems under study. Investigations of the fluence dependence and the time-of-flight spectra of the pure layers of $CH_4$, $CD_4$, and $CD_3H$ favor a resonant heating mechanism over a direct desorption process. This finding is confirmed by the studies on mixed isotope layers of $CH_4$ and $CD_4$, $CH_4$ and $CD_3H$, as well as $CD_4$ and $CD_3H$. In these systems desorption of both components is observed after resonant excitation of one of the isotopes in the layer, which cannot be explained by a direct desorption mechanism as this would lead to a selectivity in the desorption product. In addition, the dependence of the laser fluence for the mixed layers can be explained by the existence of a threshold value for the laser energy required to introduce desorption, in agreement with a resonant heating process. The energy is, however, converted locally into kinetic energy of the molecular constituents. These hot molecules then collide with neighboring unexcited molecules causing also their desorption. This in turn causes the isotopic scrambling in randomly mixed layers.

## ACKNOWLEDGMENTS

[1] T. J. Chuang, Surf. Sci. Rep. **3**, 1 (1983).

[2] T. J. Chuang and H. Seki, Phys. Rev. Lett. **49**, 382 (1982); T. J. Chuang and I. Hussla, *ibid.* **52**, 2045 (1984).

[3] T. J. Chuang, H. Seki, and I. Hussla, Surf. Sci. **158**, 525 (1985).

[4] J. Heidberg, H. Stein, and E. Riehl, Phys. Rev. Lett. **49**, 666 (1982).

[5] J. Heidberg, H. Stein, E. Riehl, Z. Szilagyi, and H. Weiss, Surf. Sci. **158**, 553 (1985).

[6] J. Heidberg, K.-W. Stahmer, H. Stein, and H. Weiss, J. Electron Spectrosc. Relat. Phenom. **45**, 87 (1987); J. Heidberg, H. Stein, and H. Weiss, Surf. Sci. Lett. **184**, L431 (1987); J. Heidberg, B. Brase, K.-W. Stahmer, and M. Suhren, Appl. Surf. Sci. **46**, 44 (1990).

[7] J. Heidberg, U. Noseck, M. Suhren, and H. Weiss, Ber. Bunsenges. Phys. Chem. **97**, 329 (1993).

[8] M. Buck and P. Hess, Chem. Phys. Lett. **158**, 486 (1989).

[9] B. Redlich, H. Zacharias, G. Meijer, and G. von Helden, Surf. Sci. **502–503**, 325 (2002).

[10] B. Redlich, H. Zacharias, G. Meijer, and G. von Helden, Phys. Chem. Chem. Phys. **4**, 3448 (2002).

[11] B. Redlich, L. van der Meer, H. Zacharias, G. Meijer, and G. von Helden, Nucl. Instrum. Methods Phys. Res. A **507**, 556 (2003).

[12] Z. W. Gortel, H. J. Kreuzer, P. Piercy, and R. Teshima, Phys. Rev. B **27**, 5066 (1983).

[13] A. Ben Ephraim, M. Folman, J. Heidberg, and N. Moiseyev, J. Chem. Phys. **89**, 3840 (1988).

[14] J. T. Muckerman and T. Uzer, J. Chem. Phys. **90**, 1968 (1989).

[15] B. Fain and Z. W. Gortel, Physica B **159**, 361 (1989).

[16] G. P. Brivio and Z. W. Gortel, Surf. Sci. **261**, 359 (1992).

[17] G. P. Brivio, M. L. Rossi, M. Torri, and Z. W. Gortel, Phys. Rev. Lett. **76**, 3376 (1996).

[18] S. A. Corcelli and J. C. Tully, J. Chem. Phys. **116**, 8079 (2002).

[19] S. A. Corcelli and J. C. Tully, J. Phys. Chem. A **106**, 10849 (2002).

[20] D. Oepts, A. F. G. van der Meer, and P. W. van Amersfoort, Infrared Phys. Technol. **36**, 297 (1995).

[21] G. Herzberg, *Infrared and Raman Spectra of Polyatomic Molecules*, Molecular Spectra and Molecular Structure Vol. II (Krieger, Malabar, FL, 1991).

[22] B. Redlich, B. Sartakov, H. Zacharias, G. Meijer, and G. von Helden (unpublished).

[23] B. N. J. Persson and R. Ryberg, Phys. Rev. B **24**, 6954 (1981).